Halogen bonding interactions with the $[Mo_3S_7Cl_6]^{2-}$ cluster anion in the mixed valence salt $[EDT\text{-}TTFI_2]_4[Mo_3S_7Cl_6]\cdot CH_3CN$†

Antonio Alberola,[a] Marc Fourmigué,*[c] Carlos J. Gómez-García,[b] Rosa Llusar*[a] and Sonia Triguero[a]

Received (in Durham, UK) 8th January 2008, Accepted 30th May 2008
First published as an Advance Article on the web 12th June 2008
DOI: 10.1039/b800298c

Electrocrystallization of iodinated TTF molecules in presence of trinuclear $[Mo_3S_7Cl_6]^{2-}$ cluster anions provides the first example of radical salts with halogen bonding interactions at the organic/inorganic interface.

Introduction

The solid state organization of molecular conductors based on partially oxidized molecules such as tetrathiafulvalene derivatives is primarily based on the overlap interaction between partially oxidized molecules, leading to low dimensional band structures with partially filled bands, hence their metallic character.[1] While the details of these overlap interactions are of paramount importance in determining the electronic properties of the salts, the chemist has a limited number of ways at their disposal to control the exact solid state organization adopted by the donor molecules and the counter ions during the electrocrystallization[2] experiments. Historically, besides modifications of the organic donors themselves,[3] the choice of counter ions of increasing complexity, with a variety of charges, volumes, connectivity and shapes, has been the driving force behind the upsurge of hundreds of new molecular conductors and superconductors.[4] In that respect, larger polyoxometalate anions ($Mo_6O_{19}^{2-}$, $PW_{12}O_{40}^{3-}$,...)[5,6] as well as polynuclear metal clusters [$(Mo_6X_8Y_6)^{2-}$,[7] $(Re_6S_{8-n}X_nY_6)^{n-4}$,...][8] have provided novel types of structural association, together with extended isostructural series where the role of embedded solvent molecules was highlighted.[9] In this context, the chemistry of trinuclear cluster anions of lower symmetry, *i.e.* $[Mo_3(\mu_3\text{-}Q)(\mu\text{-}Q_2)_3X_6]^{2-}$, with Q = S, Se, X = Cl, Br or I, incorporating one capping chalcogen atom and three bridging dichalcogenides,[10] is particularly attractive for (i) the easy substitution of the outer halide atoms by a large variety of ligands,[10–12] (ii) the interesting third-order nonlinear optical,[11] electrochemical and magnetic properties[13] introduced by ligand modifications, (iii) their successful use as electrolytes in electrocrystallization experiments with a variety of TTF derivatives such as BEDT-TTF [bis(ethylenedithio)tetrathiafulvalene] with $[Mo_3S_7Br_6]^{2-}$ and $[Mo_3S_7Cl_6]^{2-}$.[14]

At this stage however, as in most electrocrystallization experiments so far, we have no control over the obtained solid state structures and particularly over the organic/inorganic interface. Actually, earlier reports on the role of weak C–H···O,N,X hydrogen bonds in BEDT-TTF salts[5,15] have prompted an increasing effort to specifically modify this interface, by introducing on the TTF core functional groups able to recognize a specific site on the anionic layers. This was primarily addressed with the intentional use of normal *hydrogen bonds*,[16,17] by substituting the TTF core with hydrogen bond donor groups such as alcohols,[18] acids[19] or amides.[20,21] In a parallel way, Kato introduced in 1995 another intermolecular interaction to control the organic/inorganic interface of molecular conductors,[22] which is the halogen bond.[23,24] This interaction between an organic halide acting as halogen bond *donor* and a halogen as a bond *acceptor* (halogen atoms themselves being Lewis bases) is based on the anisotropy of the electron density around the halogen atom, which leads to (i) a smaller effective radius along the extended C–X bond axis than in the perpendicular direction, (ii) an electron-deficient region (+δ) along this C–X axis, acting as electrostatic attractive potential toward Lewis bases. This interaction leads to a number of specific structural motifs, such as a linear motif with the lone pairs of a nitrile or a pyridine, and type I or type II motifs for interactions between halogens (Scheme 1).[25]

According to this concept,[17] halogenated TTFs such as EDT-TTF-I or EDT-TTF-I_2 were successfully electrocrystallized with various halo anions such as Br^-,[22,26] I^-,[27] IBr_2^-,[28] $Pb_{5/6}I_2^-$,[29] cyano anions such as $[Ag(CN)_2]^-$ or[22] $[Au(CN)_4]^-$,[30] and nitrile-containing dithiolene anions such as $[Ni(mnt)_2]^-$.[31] The halogen bonding was not only observed in these salts but was even enhanced due to the activation of the +δ character of the halogen atom bonded to the TTF core when the TTF is oxidized to the cation radical.[17]

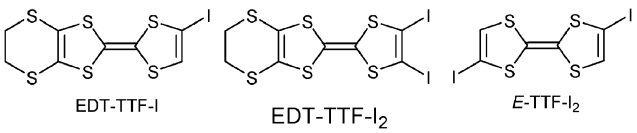

At that point, it was tempting to associate the variability of shape and size of large cluster anions evoked above with

[a] *Departament de Química Física i Analítica, Universitat Jaume I, Avda. Sos Baynat s/n, E-12071 Castelló, Spain*
[b] *Instituto de Ciencia Molecular, Universitat de Valencia, Polígono la Coma s/n, E-46980 Paterna, Spain*
[c] *Sciences Chimiques de Rennes, Université Rennes 1, UMR CNRS 6226, Campus de Beaulieu, F-35042 Rennes, France*

† Electronic supplementary information (ESI) available: Crystallographic data in CIF format. CCDC reference number 689245. See DOI: 10.1039/b800298c

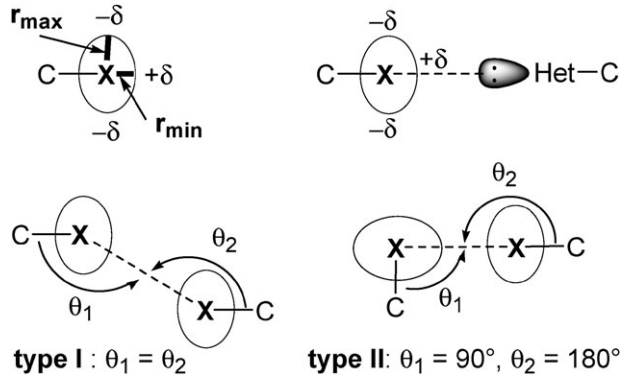

Scheme 1 Top: anisotropic electron distribution around the halogen atom (left) and interaction with a Lewis base (right). Bottom: Hal···Hal bonding patterns.

the efficiency of the halogen bonding interaction to control the organic/inorganic interface with such counter ions. This was first recently addressed by Batail *et al.* who reported the electrocrystallization of iodotetrathiafulvalene derivatives with the hexanuclear $[Re_6Se_8(CN)_6]^{4-}$ cluster anion.[32] In the salt reported with *E*-TTF-I_2 for example, two *trans* cyanide moieties of $[Re_6Se_8(CN)_6]^{4-}$ associate with $(E\text{-TTF-}I_2)^{+\bullet}$ to afford polymeric chains through strong halogen bonds, but at the expense of the organic/inorganic segregation needed for overlap interaction between the cation radical species, probably because of the symmetrical nature of the cluster anion and the highly directional C–I···NC interaction.

We report here that the use of a cluster anion of lower symmetry such as $[Mo_3S_7Cl_6]^{2-}$ allows for the successful electrocrystallization of mixed-valence salts of iodinated TTFs, with the simultaneous occurrence of: (i) strong halogen bonds at the organic/inorganic interface and (ii) a two-dimensional segregation of the partially oxidized TTF cation radicals in the conducting salt $[EDT\text{-}TTF\text{-}I_2]_4[Mo_3S_7Cl_6]\cdot CH_3CN$. This provides the very first example of halogen bonding interactions at the organic/inorganic interface in TTF salts with complex polymetallic cluster anions.

Results and discussion

The electrocrystallization of EDT-TTF-I_2 was attempted with several trimetallic cluster anions such as $[Mo_3S_7Cl_6]^{2-}$, $[Mo_3S_7Br_6]^{2-}$ and $[Mo_3S_7(SCN)_6]^{2-}$. Black polycrystalline material was obtained in most cases. However, performing the electrocrystallizations at higher temperatures (+40 °C) afforded, in the presence of $(^nBu_4N)_2[Mo_3S_7Cl_6]$ small single crystals on the anode. The salt crystallizes in the triclinic system, space group $P\bar{1}$ with four crystallographically independent donor molecules, one $[Mo_3S_7Cl_6]^{2-}$ counter ion and one acetonitrile solvent molecule, all of them in general positions in the unit cell (Fig. 1), which corresponds thus to a $[EDT\text{-}TTF\text{-}I_2]_4[Mo_3S_7Cl_6]\cdot CH_3CN$ formula.†

It is therefore a mixed valence salt, potentially conducting. The intramolecular bond distances within the TTF core of the partially oxidized donor molecules are collected in Table 1, together with some reference compounds. We note that the central C=C and C–S bonds exhibit large variations between the four crystallographically independent molecules, possibly indicating a variable degree of oxidation among the four molecules. Evaluation of charge transfer can be performed based on the Coppens formulae[33] which relates the degree of charge transfer ρ to either the ratio (C=C)/(C–S) or the difference (C=C) − (C–S) with $\rho_{ratio} = A + B\cdot$(C=C)/(C–S) or $\rho_{diff.} = C + D\cdot$[(C=C) − (C–S)], respectively. Such correlations have been successfully used in TTF[33] as well as BEDT-TTF salts.[34] A linear fit with the published data for the neutral EDT-TTF-I ($\rho = 0$) and the salts $(EDT\text{-}TTF\text{-}I_2)_2I_3$ and $(EDT\text{-}TTF\text{-}I_2)I_3$ with $\rho = 0.5$ and 1, respectively, afforded the following values: $A = -12.221$, $B = +16.223$, $C = +3.7148$ and $D = +8.5462$. Using those values for our salt we can obtain an estimation of the different degrees of charge transfer for the four independent EDT-TTF-I_2 donor molecules. Thus, molecule A is essentially neutral while molecules B, C and D share the 2+ oxidation state.

In the solid state (Fig. 1), we observe the typical segregation of the organic (EDT-TTFI_2) moieties on the one hand and the inorganic/solvent moieties on the other. As shown in Fig. 2, the organic/inorganic interface is characterized by numerous

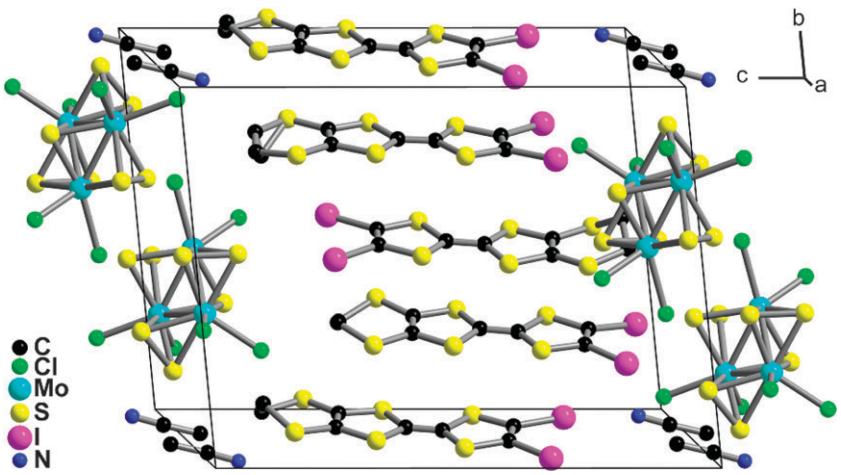

Fig. 1 A view of the four crystallographically independent EDT-TTFI_2 molecules in $[EDT\text{-}TTF\text{-}I_2]_4[Mo_3S_7Cl_6]\cdot CH_3CN$, showing also the organic/inorganic segregation and the interstitial CH_3CN molecules embedded in the inorganic layers.

Table 1 Bond lengths (Å) and estimation of the degree of charge transfer (ρ) (see text) in EDT-TTF-I_2 derivatives

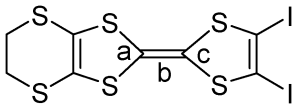

	C–S bond a	C–S bond c	(C–S)av.	C=C bond b	ρ_{ratio}	$\rho_{diff.}$	ρ	Ref.
Molecule A	1.762(16) 1.752(20)	1.761(20) 1.745(16)	1.755	1.335(23)	+0.12	+0.12		This work
Molecule B	1.723(15) 1.731(18)	1.756(19) 1.743(15)	1.738	1.393(22)	+0.78	+0.77		This work
Molecule C	1.722(16) 1.708(13)	1.731(14) 1.743(19)	1.726	1.378(21)	+0.73	+0.74		This work
Molecule D	1.727(14) 1.734(18)	1.738(17) 1.720(14)	1.730	1.373(21)	+0.65	+0.66		This work
$\Sigma\rho$					+2.28	+2.29		
EDT-TTF-I	[a]	[a]	1.763	1.332(13) 1.324(14)			0	31*b*
$(EDT\text{-}TTF\text{-}I_2)_2I_3$	1.733(24) 1.741(19)	1.731(20) 1.757(24)	1.740	1.365(29)			0.5	28
$(EDT\text{-}TTF\text{-}I_2)I_3$	1.718(9)	1.718(9)	1.718	1.40(2)			1	35

[a] Two crystallographically independent molecules.

halogen bonding interactions which settle between the iodine atoms of the partially oxidized A–D molecules and as "acceptor" atoms, six chlorine atoms and one sulfur atom of the $[Mo_3S_7Cl_6]^{2-}$ cluster anions and the nitrogen atom of the acetonitrile solvent molecule, firmly embedded in the inorganic layer. The structural characteristics on these halogen interactions (Table 2) confirm their bonding nature as the I···(Cl, N) distances are far shorter than the sum of van der Waals radii, but also shorter than the D_{max} distances determined according to Nyburg by taking into account the non-spherical shape of the atoms.[36] All, except that with the sulfur atom, exhibit a strong linearity characteristic of halogen bonding.

The organic slabs are formed by parallel stacks related to each other by inversion. Within a given organic stack (Fig. 3), we observe an ACBDACBD alternation, with the iodine atoms of the A, C and D molecules pointing in one direction, and those of the B molecule in the other direction.

The four possible overlap interactions within these stacks, that is BD, BC, AC and AD are shown in Fig. 4. We observe that BC and BD involve a head-to-tail overlap while AC and AD associate molecules with the same orientation.

From the calculations of the charge on each donor molecule (see above) we can assume that the charge on molecule A is essentially zero while molecules B, C and D share the +2 charge. Thus, the stacks can be tentatively described as follows: $-A^0-[C/B/D]^{2+}-A^0-[C/B/D]^{2+}-$, with a head-to-tail overlap within the $[C/B/D]^{2+}$ trimer and a head-to-head overlap with the almost neutral A^0. Based on this description of almost isolated dicationic trimers, the salt should be insulating or a poor semiconductor. In fact, the temperature

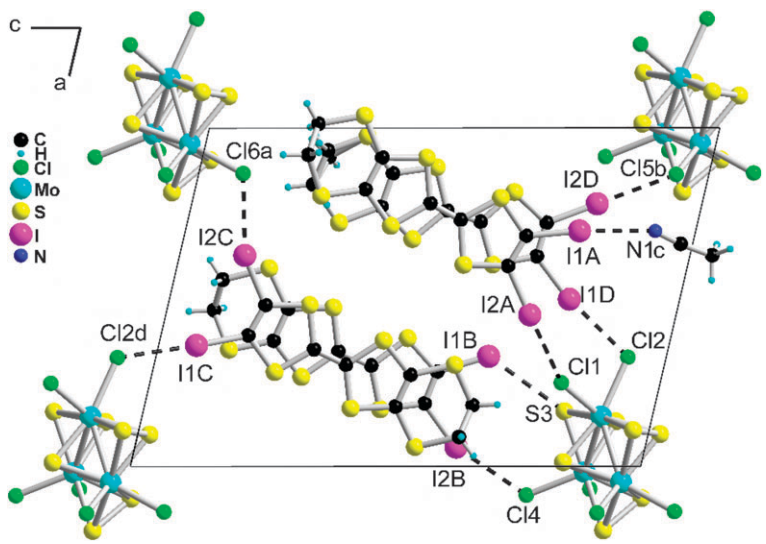

Fig. 2 Detail of the halogen bonding interactions (dotted lines), between the four crystallographically independent EDT-$TTFI_2$ molecules and neighboring atoms. Symmetry operations applied to some acceptor atoms are as follows: for Cl6, Cl6a ($-1 + x,y,1 + z$); for Cl5, Cl5b at ($-1 + x,y,z$), for N1, N1c at ($x,1 + y,z$), for Cl2, Cl2d ($x,y,1 + z$).

Table 2 Structural characteristics of the halogen bonded systems, where D_{max} is the contact distance for a type II interaction, determined[a] from the sum of the non-spherical van der Waals radii.[36] See Fig. 2 for the atom numbering and symmetry operations

Interaction	I···X/Å	D_{max}/Å	C–I···X/°
I1A···N1c	2.98(2)	3.36	171.7(6)
I2A···Cl1	3.563(5)	3.54	151.0(5)
I1B···S3	3.609(6)	3.79	127.5(4)
I2B···Cl4	3.273(5)	3.54	158.2(5)
I1C···Cl2d	3.278(5)	3.54	171.5(4)
I2C···Cl6a	3.168(4)	3.54	158.3(4)
I1D···Cl2	3.172(5)	3.54	171.3(4)
I2D···Cl5b	3.245(5)	3.54	168.9(4)

[a] See Table 13 in ref. 17*a*.

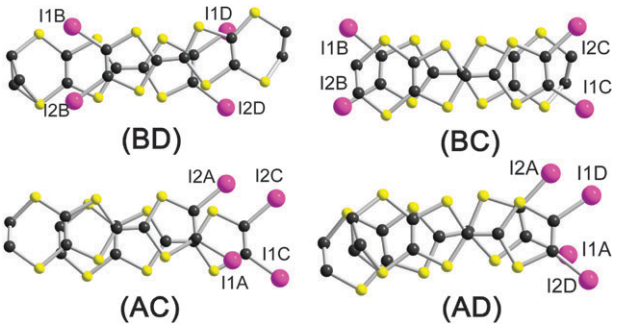

Fig. 4 Overlap patterns within the stacks.

dependence of the dc electrical conductivity, determined on two different single crystals, shows that the title compound exhibits semiconducting behavior with a low room temperature conductivity of *ca.* 10^{-4} S cm^{-1} and two different semiconducting regimes, both with high activation energies of *ca.* 290 meV (between 300 and 265 K) and 230 meV (between 265 and 240 K). Below 240 K the resistivity is too high to be measured by our conductimeter. In order to understand this behavior, we have also determined for every bimolecular interaction the HOMO–HOMO overlap interaction energies (H_{ij}) from tight binding extended Hückel calculations (see Fig. 3).[37,38] For the interaction along the stacks, we obtained for H_{ac}, H_{bc}, H_{bd} and H_{ad}, 0.288, 0.430, 0.216 and 0.412 eV, respectively. The interactions between stacks are much weaker, since we found for H_{aa}, H_{bb}, H_{cd1}, H_{cd2}, H_{act}, H_{bdt}, H_{adt} and H_{bct}, respectively 0.046, 0.087, 0.020, 0.045, 0.00, 0.012; 0.125 and 0.007 eV. The existence of two different semiconducting regimes with faint transitions near room temperature has already been observed in other radical salts of ET-type donors and may be attributed to the ordering of the ethylene group of the EDT-TTFI$_2$ molecule.[14*b*,39]

To corroborate these observations, magnetic susceptibility measurements were performed on a polycrystalline sample. As can be seen in Fig. 5, the broad maximum in the susceptibility indicates low-dimensional antiferromagnetic exchange, while the fact that the susceptibility tends to 0 at $T = 0$ K suggests a system with a magnetic gap. It is therefore possible that Coulomb repulsion is large and therefore the spins are localized into the $[C/B/D]^{2+}$ trimeric moieties, hence the low conductivity of the salt.[40] To model the observed behavior, a singlet–triplet model[41] was examined. A term to account for the Curie contribution, clearly visible at low temperatures, arising from paramagnetic impurities and defects in the sample was also included in the fitting routine. This model reproduces satisfactorily the magnetic data with a S–T gap for the dimer, $2J = -196(5)$ cm^{-1}, $g = 2.05(3)$ and 3.5(1)% of monomeric paramagnetic impurity (dashed line in Fig. 5). Although this model reproduces quite well the overall magnetic behavior, the minimum at *ca.* 50 K is not well reproduced. This result indicates that there must be an extra magnetic coupling between the $[C/B/D]^{2+}$ trimeric units. To account for this extra coupling, we have used a model of interacting dimers by means of the molecular field approximation:[42]

$$\chi^{*}_{dim} = \frac{\chi_{dim}}{1 - (2zJ^{*}/Ng^{2}\beta^{2})\chi_{dim}}$$

where J^* is the inter-dimer exchange constant, z is the number of neighbors (which is assumed to be two) and χ_{dim} is the

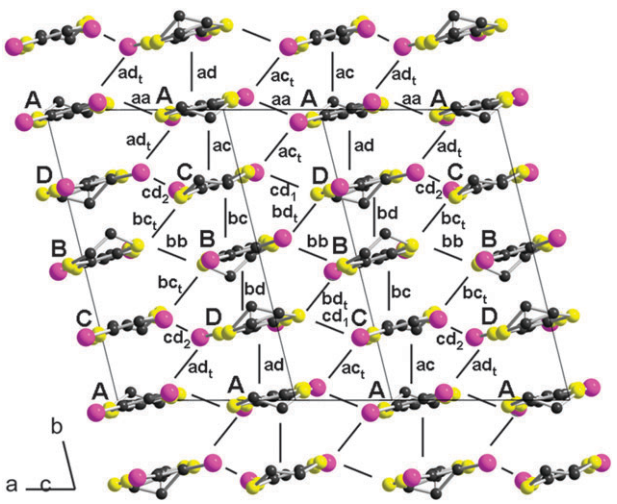

Fig. 3 A view of the organic slab (black lines indicate the intermolecular interactions).

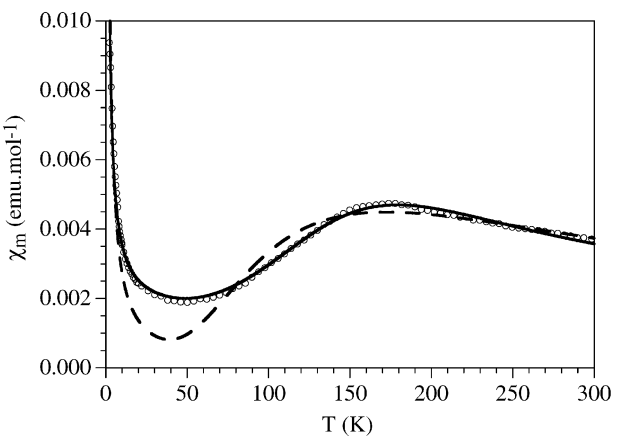

Fig. 5 Thermal variation of the magnetic susceptibility of the title compound. The dotted line is the best fit to a simple dimer model. The continuous line is the best fit to a model of interacting dimers (see text).

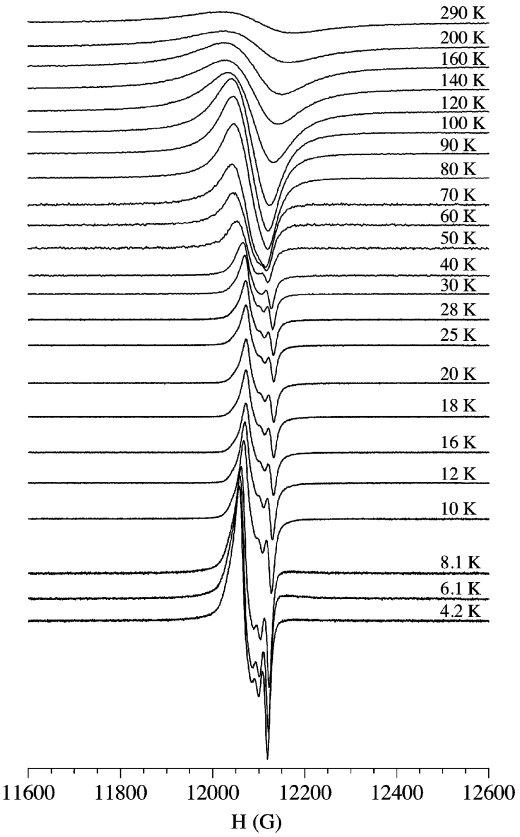

Fig. 6 Q-Band EPR spectra of the title compound at different temperatures.

susceptibility of the singlet–triplet model. This model reproduces very satisfactorily the magnetic data in the whole temperature range, including the minimum at *ca.* 50 K with the following parameters: $g = 2.01(6)$, $2J = -201(2)$ cm^{-1}, $J^* = -84(3)$ cm^{-1} and a 4.4(3)% of monomeric paramagnetic impurity (solid line in Fig. 5). The similarity in the values of the two exchange parameters is in agreement with the also similar calculated HOMO/HOMO overlap interaction energies (see above). Thus, each $[C/B/D]^{2+}$ trimeric unit interacts with the two neighboring $[C/B/D]^{2+}$ trimeric units in adjacent chains, with overall interaction energies of 191 eV ($2^*H_{cd2} + 2^*H_{bct} + H_{bb}$) and 0.151 eV ($2^*H_{cd1} + 2^*H_{bdt} + H_{bb}$) (see Fig. 3), of the same order as the values found inside the $[C/B/D]^{2+}$ trimeric unit (0.216 and 0.430 eV).

The thermal variation of the EPR spectra of the title compound is very similar to that of the BEDT-TTF salt of the same anion[14b] and confirms the results obtained with the SQUID magnetic susceptibility measurements. Thus, at room temperature, the EPR spectrum shows a broad slightly anisotropic Lorentzian line at $g = 2.002$ with a line width of *ca.* 155 G (Fig. 6) that can be attributed to the EDT-TTFI$_2$ molecules. This anomalous large line width indicates that the spin relaxation time in the organic sublattice must be very short, suggesting the presence of effective relaxation pathways through the many I···Cl and I···S interactions observed between the organic and inorganic sublattices (see above). In fact, in two dimensional radical salts of the TTF type the line widths are about one half that of the title compound (usually

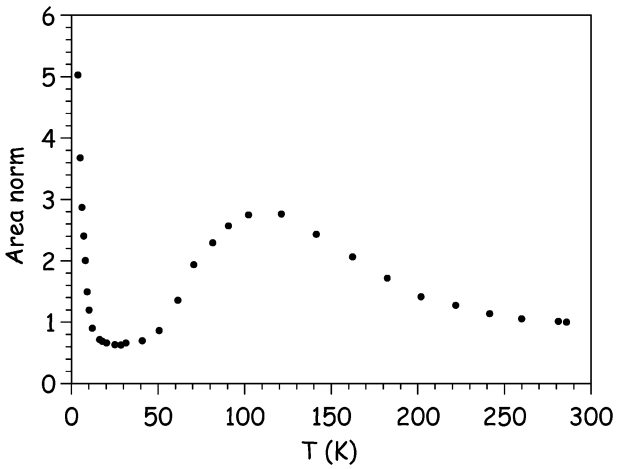

Fig. 7 Normalized temperature dependence of the spin susceptibility obtained from the area of the EPR signal.

in the range 40–80 G).[43] When lowering the temperature the line narrows down to *ca.* 70 G at 70 K. Below this temperature the signal splits into two lines and below *ca.* 30 K up to three lines, typical of a rhombic spectrum, can be observed. This splitting of the donor signal into three separate components is very unusual in this kind of radical salts and, as far as we know, has only been observed very recently in two radical salts, both with the donor BEDT-TTF and also with bulky anions.[14b,44]

The intensity of the signal increases when lowering the temperature down to *ca.* 120 K. Below this temperature the intensity of the signal decreases, reaching a minimum at *ca.* 40 K to increase again below this temperature (Fig. 7). This behavior parallels the SQUID magnetic susceptibility measurements (Fig. 5) and confirms the presence of a strong antiferromagnetic coupling in the organic sublattice as well as a small amount of paramagnetic impurities associated to isolated donor molecules.

Conclusions

The title compound represents one of the very scarce examples of radical salts presenting a true interaction between the organic and inorganic sub-lattices. In fact, as far as we know, the title compound presents the largest line width of an EPR signal observed to date in a TTF-type radical salt, indicating the presence of strong interactions through the numerous I···Cl and I···S short contacts observed in the structure of the title compound. This interaction is the result of the presence of two iodine atoms in the donor molecules and several accessible acceptor atoms such as Cl and S in the anion and demonstrates the feasibility of this kind of TTF-type donors to prepare hybrid molecular materials with interactions between the two sublattices.

Experimental

Electrocrystallization experiments. The donor molecule EDT-TTFI$_2$ and the electrolyte (^{n}Bu$_4$N)$_2$(Mo$_3$S$_7$Cl$_6$) were prepared as previously described. Electrocrystallization was performed

with EDT-TTFI$_2$ (10 mg) and (^{n}Bu$_4$N)$_2$(Mo$_3$S$_7$Cl$_6$) (40 mg) in a CH_3CN solution (10 mL) containing CH_2Cl_2 (0.5 mL) to help the dissolution of EDT-TTFI$_2$. Constant current of 0.5 μA was applied during two weeks on Pt electrodes (length 2 cm, diameter 0.1 cm) while the cell was thermostated at 40 °C.

Crystallography. The crystal was mounted on the top of a thin glass fiber with Araldite® glue. Data were collected on a Nonius KappaCCD Diffractometer at room temperature with graphite-monochromated Mo-Kα radiation (λ = 0.71073 Å). The structure was solved by direct methods (SHELXS-97) and refined (SHELXL-97)[45] by full-matrix least-squares methods, as implemented in the WinGX software package.[46] Absorption correction was applied. Hydrogen atoms were introduced at calculated positions (riding model), included in structure factor calculations, and not refined. Crystal data for (EDT-TTFI$_2$)$_4$(Mo$_3$S$_7$Cl$_6$)(CH$_3$CN): $C_{34}H_{19}Cl_6I_8Mo_3NS_{31}$, M = 2951.08, space group $P\bar{1}$, a = 13.6879(4), b = 14.8842(3), c = 20.1813(5) Å, α = 76.2650(10), β = 74.578(2), γ = 78.0550(10)°, V = 3804.53(16) Å^3, Z = 2, D_{calcd} = 2.576 g cm^{-3}, μ = 4.827 mm^{-1}; 63 914 reflections collected, 17 437 independent (R_{int} = 0.1269) and 7708 with $I > 2\sigma(I)$. 742 parameters refined to give $R(F)$ = 0.0624 and $R_w(F^2)$ = 0.2348.

Conductivity measurements. Conductivity measurements over the range 2–300 K were performed with the standard four contacts method on single crystals in a Quantum Design PPMS-9. Contacts to the samples were made by platinum wires (25 μm diameter) attached by graphite paste to the samples. The cooling and warming rate was in the range 0.25–0.5 K min^{-1} and the intensity of the applied DC current was in the range 0.01–1.0 μA.

Magnetic properties. Magnetic susceptibility measurements were made on a Quantum Design SQUID magnetometer in an applied field of 100 G between 3 K and 300 K on 2.5 mg of polycrystalline sample. Data were corrected for both sample diamagnetism (Pascal's constants) and the sample holder. Q-Band ESR spectra were recorded on a polycrystalline sample with a Bruker E-500 ELEXSYS spectrometer in the temperature range 300–4.2 K.

Acknowledgements

This work was made possible through the support of the French Spanish Integrated Action program PICASSO (no 11445PL), the Spanish Ministerio de Educación y Ciencia (Project CSD 2007-00010 Consolider-Ingenio in Molecular Nanoscience and CTQ 2005-09270-C02-1), the EU (COST action D35-0011) and Generalitat Valenciana (Grant ACOMP/2007/286). S.T. thanks Fundació Caixa Castelló-Bancaixa support for her stay at Université de Rennes. A.A. thanks the Spanish Ministerio de Educación y Ciencia for a Ramón y Cajal research contract.

References

1. See the special *Chem. Rev.* issue on *Molecular Conductors*, ed. P Batail, *Chem. Rev.*, 2004, **11**, 104.
2. P. Batail, K. Boubekeur, M. Fourmigué and J.-C. P. Gabriel, *Chem. Mater.*, 1998, **10**, 3005.
3. (*a*) J. Yamada, H. Akutsu, H. Nishikawa and K. Kikuchi, *Chem. Rev.*, 2004, **104**, 5057; (*b*) M. Iyoda, M. Hasegawa and Y. Miyake, *Chem. Rev.*, 2004, **104**, 5085; (*c*) J. M. Fabre, *Chem. Rev.*, 2004, **104**, 51433; (*d*) D. Lorcy and N. Bellec, *Chem. Rev.*, 2004, **104**, 5185.
4. (*a*) E. Coronado and P. Day, *Chem. Rev.*, 2004, **104**, 5419; (*b*) U. Geiser and J. A. Schlueter, *Chem. Rev.*, 2004, 5203.
5. A. Davidson, K. Boubekeur, A. Pénicaud, P. Auban, C. Lenoir, P. Batail and G. Hervé, *J. Chem. Soc., Chem. Commun.*, 1989, 1373.
6. E. Coronado and C. J. Gómez-García, *Chem. Rev.*, 1998, **98**, 273.
7. P. Batail, C. Livage, S. S. P. Parkin, C. Coulon, J. D. Martin and E. Canadell, *Angew. Chem., Int. Ed. Engl.*, 1991, **30**, 1498.
8. J.-C. P. Gabriel, K. Boubekeur, S. Uriel and P. Batail, *Chem. Rev.*, 1999, **9**, 2173.
9. (*a*) A. Deluzet, R. Rousseau, C. Guilbaud, I. Granger, K. Boubekeur, P. Batail, E. Canadell, P. Auban-Senzier and D. Jerome, *Chem.–Eur. J.*, 2002, **8**, 3884; (*b*) A. Deluzet, P. Batail, Y. Misaki, P. Auban-Senzier and E. Canadell, *Adv. Mater.*, 2000, **12**, 436; (*c*) A. Pénicaud, K. Boubekeur, P. Batail, E. Canadell, P. Auban-Senzier and D. Jérome, *J. Am. Chem. Soc.*, 1993, **115**, 4101.
10. V. Bereau, C. G. Pernin and J. A. Ibers, *Inorg. Chem.*, 2000, **39**, 854.
11. J. M. Garriga, R. Llusar, S. Uriel, C. Vicent, A. J. Usher, N. T. Lucas, M. G. Humphrey and M. Samoc, *Dalton Trans.*, 2003, 4546.
12. V. P. Fedin, M. N. Sokolov, V. Y. Fedorov, D. S. Yufit and Y. T. Struchkov, *Inorg. Chim. Acta*, 1991, **179**, 35.
13. R. Llusar, S. Uriel, C. Vicent, E. Coronado, C. J. Gomez-Garcia, J. M. Clemente-Juan, B. Braida and E. Canadell, *J. Am. Chem. Soc.*, 2004, **126**, 12076.
14. (*a*) R. Llusar, S. Triguero, S. Uriel, C. Vicent, E. Coronado and C. J. Gomez-Garcia, *Inorg. Chem.*, 2005, **44**, 1563; (*b*) A. Alberola, R. Llusar, S. Triguero, C. Vicent, M. N. Sokolov and C. J. Gomez-Garcia, *J. Mater. Chem.*, 2007, **17**, 3440.
15. M. H. Wangbo, J. M. Williams, A. J. Schultz, T. J. Emge and M. A. Beno, *J. Am. Chem. Soc.*, 1987, **109**, 90.
16. M. R. Bryce, *J. Mater. Chem.*, 1995, **5**, 1481.
17. (*a*) M. Fourmigué and P. Batail, *Chem. Rev.*, 2004, **104**, 5379; (*b*) M. Fourmigué, *Struct. Bonding*, 2008, **126**, 181.
18. (*a*) P. Blanchard, K. Boubekeur, M. Sallé, G. Duguay, M. Jubault, A. Gorgues, J. D. Martin, E. Canadell, P. Auban-Senzier, D. Jérome and P. Batail, *Adv. Mater.*, 1992, **4**, 579; (*b*) A. Dolbecq, M. Fourmigué, P. Batail and C. Coulon, *Chem. Mater.*, 1994, **6**, 1413; (*c*) A. Dolbecq, A. Guirauden, M. Fourmigué, K. Boubekeur, P. Batail, M. M. Rohmer, M. Bénard, C. Coulon, M. Sallé and P. Blanchard, *J. Chem. Soc., Dalton Trans.*, 1999, 1241.
19. A. Dolbecq, M. Fourmigué, F. C. Krebs, P. Batail, E. Canadell, R. Clérac and C. Coulon, *Chem.–Eur. J.*, 1996, **2**, 1275.
20. (*a*) K. Heuzé, M. Fourmigué, P. Batail, E. Canadell and P. Auban-Senzier, *Chem.–Eur. J.*, 1999, **5**, 2971; (*b*) K. Heuzé, C. Mézière, M. Fourmigué, P. Batail, C. Coulon, E. Canadell, P. Auban-Senzier and D. Jérome, *Chem. Mater.*, 2000, **12**, 1898.
21. (*a*) S. A. Baudron, N. Avarvari, P. Batail, C. Coulon, R. Clérac, E. Canadell and P. Auban-Senzier, *J. Am. Chem. Soc.*, 2003, **125**, 11583; (*b*) S. A. Baudron, N. Avarvari, E. Canadell, P. Auban-Senzier and P. Batail, *Chem.–Eur. J.*, 2004, **10**, 4498.
22. T. Imakubo, H. Sawa and R. Kato, *Synth. Met.*, 1995, **73**, 117.
23. (*a*) W. Jones, C. R. Theocharis, J. M. Thomas and G. R. Desiraju, *J. Chem. Soc., Chem. Commun.*, 1983, 1443; (*b*) T. Sakurai, M. Sundaralingam and G. A. Jeffrey, *Acta Crystallogr.*, 1963, **16**, 354; (*c*) S. C. Nyburg and W. Wong-Ng, *Proc. R. Soc. London, Ser. A*, 1979, **367**, 29; (*d*) D. E. Williams and L. Y. Hsu, *Acta Crystallogr., Sect. A: Found. Crystallogr.*, 1985, **41**, 296; (*e*) G. R. Desiraju and R. Parthasarathy, *J. Am. Chem. Soc.*, 1989, **111**, 8725; (*f*) S. L. Price, A. L. Stone, J. Lucas, R. S. Rowland and A. E. Thornley, *J. Am. Chem. Soc.*, 1994, **116**, 4910; (*g*) O. Navon, J. Bernstein and V. Khodorkovsky, *Angew. Chem., Int. Ed. Engl.*, 1997, **36**, 601; (*h*) V. R. Pedireddi, D. S. Reddy, B. S. Goud, D. C. Craig, A. D. Rae and G. R. Desiraju, *J. Chem. Soc., Perkin Trans. 2*, 1994, 2353.
24. (*a*) P. Metrangolo and G. Resnati, *Chem.–Eur. J.*, 2001, **7**, 2511; (*b*) E. Corradi, S. V. Meille, M. T. Messina, P. Metrangolo and G. Resnati, *Angew. Chem., Int. Ed.*, 2000, **39**, 1782; (*c*) T. Caronna, R. Liantonio, T. A. Logothetis, P. Metrangolo, T. Pilati and G. Resnati, *J. Am. Chem. Soc.*, 2004, **126**, 4500.

25. (*a*) P. Metrangolo, H. Neukirch, T. Pilati and G. Resnati, *Acc. Chem. Res*., 2005, **38**, 386; (*b*) C. M. Reddy, M. T. Kirchner, R. C. Gundakaram, K. A. Padmanabhan and G. R. Desiraju, *Chem.–Eur. J*., 2006, **12**, 2222; (*c*) F. Zordan, L. Brammer and P. Sherwood, *J. Am. Chem. Soc*., 2005, **127**, 5979.
26. T. Imakubo, T. Shirahata, K. Kervé and L. Ouahab, *J. Mater. Chem*., 2006, **16**, 162.
27. R. Gompper, J. Hock, K. Polborn, E. Dormann and H. Winter, *Adv. Mater*., 1995, **7**, 41.
28. B. Domercq, T. Devic, M. Fourmigué, P. Auban-Senzier and E. Canadell, *J. Mater. Chem*., 2001, **11**, 1570.
29. T. Devic, M. Evain, Y. Moëlo, E. Canadell, P. Auban-Senzier, M. Fourmigué and P. Batail, *J. Am. Chem. Soc*., 2003, **125**, 3295.
30. T. Imakubo, A. Miyake, H. Sawa and R. Kato, *Synth. Met*., 2001, **120**, 927.
31. (*a*) J. Nishijo, E. Ogura, J. Yamaura, A. Miyazaki, T. Enoki, T. Takano, Y. Kuwatani and M. Iyoda, *Solid State Commun*., 2000, **116**, 661; (*b*) T. Devic, B. Domercq, P. Auban-Senzier, P. Molinié and M. Fourmigué, *Eur. J. Inorg. Chem*., 2002, 2844.
32. A. Ranganathan, A. El-Ghayoury, C. Mézière, E. Harté, R. Clérac and P. Batail, *Chem. Commun*., 2006, 2878.
33. T. C. Umland, S. Allie, T. Kuhlmann and P. Coppens, *J. Phys. Chem*., 1988, **92**, 6456.
34. P. Guionneau, C. J. Kepert, D. Chasseau, M. R. Truter and P. Day, *Synth. Met*., 1997, **86**, 1973.
35. T. Devic and M. Fourmigué, unpublished results.
36. S. C. Nyburg and C. H. Faerman, *Acta Crystallogr., Sect. B: Struct. Sci*., 1985, **41**, 274.
37. M. H. Whangbo and R. Hoffmann, *J. Am. Chem. Soc*., 1978, **100**, 6093.
38. J. Ren, W. Liang and M. H. Whangbo, *Crystal and Electronic Structure Analysis Using CAESAR*, Prime Coloror Software Inc., North Carolina, USA, 1998.
39. E. Coronado, S. Curreli, C. Giménez-Saiz and C. J. Gómez-García, *J. Mater. Chem*., 2005, **15**, 1429.
40. S. D. Obertelli, R. H. Friend, D. R. Talham, M. Kurmoo and P. Day, *J. Phys.: Condens. Matter*, 1989, **1**, 5671.
41. B. Bleaney and K. D. Bowers, *Proc. R. Soc. London, Ser. A*, 1952, **214**, 451.
42. C. J. O'Connor, *Prog. Inorg. Chem*., 1982, **29**, 203.
43. J. M. Williams, J. R. Ferraro, R. J. Thorn, K. D. Carlson, U. Geiser, H. H. Wang, A. M. Kini and M. H. Whangbo, *Organic Superconductors. Synthesis, Structure, Properties and Theory*, ed. R. N. Grimes, Prentice Hall, Engelwood Cliffs, New Jersey, 1992.
44. M. Clemente-León, E. Coronado, C. J. Gómez-Garcia, V. N. Lauhkin, A. Soriano-Portillo, S. Constant, R. Frantz and J. Lacour, *Inorg. Chim. Acta*, 2006, **360**, 955.
45. G. M. Sheldrick, SHELX97-Programs for Crystal Structure Analysis (Release 97-2) , 1998.
46. L. J. Farrugia, *J. Appl. Crystallogr*., 1999, **32**, 837.